

EXPERIMENTAL STUDY

Anti-proliferative effects of beta-blocker propranolol on human lung cancer and noncancer cells

Menderes Yusuf TERZI^{1,2}, Meral URHAN-KUCUK^{1,2}

Hatay Mustafa Kemal University Faculty of Medicine Department of Medical Biology, Tayfur Ata Sökmen Campus, Antakya-Hatay, Turkey. menderesyusufterzi@gmail.com

ABSTRACT

OBJECTIVE: Propranolol (PRO) has been recently discovered to possess anti-tumorigenic effects in cancer patients. So, we aimed to enlighten the *in vitro* effects of PRO in A549 lung cancer cells and BEAS2B nontumoral lung cells.

METHODS: The gene expression levels of apoptotic proteins; caspases 3, 8, and 9 (CASP3, 8, 9), apoptosis inducing factor (AIF), and DNA damage inducible transcript 3 (DDIT3) and cell cycle regulatory proteins; WEE1 G2 checkpoint kinase (WEE1) and cyclin dependent kinase inhibitor 1A (CDKN1A) were analyzed with quantitative reverse-transcription PCR to assess the effect of PRO on A549 tumor and BEAS2B nontumoral cells. The protein levels of CASP3 and AIF1 were detected with Western blot.

RESULTS: PRO exerted its anti-tumorigenic effects against A549 cells by arresting cell cycle via *CDKN1A* and by inducing apoptosis via caspase-dependent (CASP3) and -independent pathways (AIF, *DDIT3*). As to nontumoral BEAS2B cells, PRO decreased the cell viability at a lesser extent compared to tumoral cells. In contrast to tumor cells, PRO reduced the protein levels of CASP3 and AIF1. Notably, at 48th hour of PRO treatment, we observed a sustained expression of elevated *DDIT3* mRNA levels at 24h in BEAS2B cells unlike in A549 cells.

CONCLUSION: We suggest that *DDIT3* and *CDKN1A* play a critical role during cell fate decision after PRO treatment by protecting nontumoral cells against apoptosis and by triggering apoptosis in tumor cells. The selective action mechanism of PRO with less cytotoxicity in nontumoral lung cells puts it forward as a promising adjuvant agent in lung cancer therapy (*Tab. 1, Fig. 4, Ref. 50*). Text in PDF www.elis.sk

KEY WORDS: propranolol, BEAS2B, A549, lung cancer, apoptosis, DDIT3.

Introduction

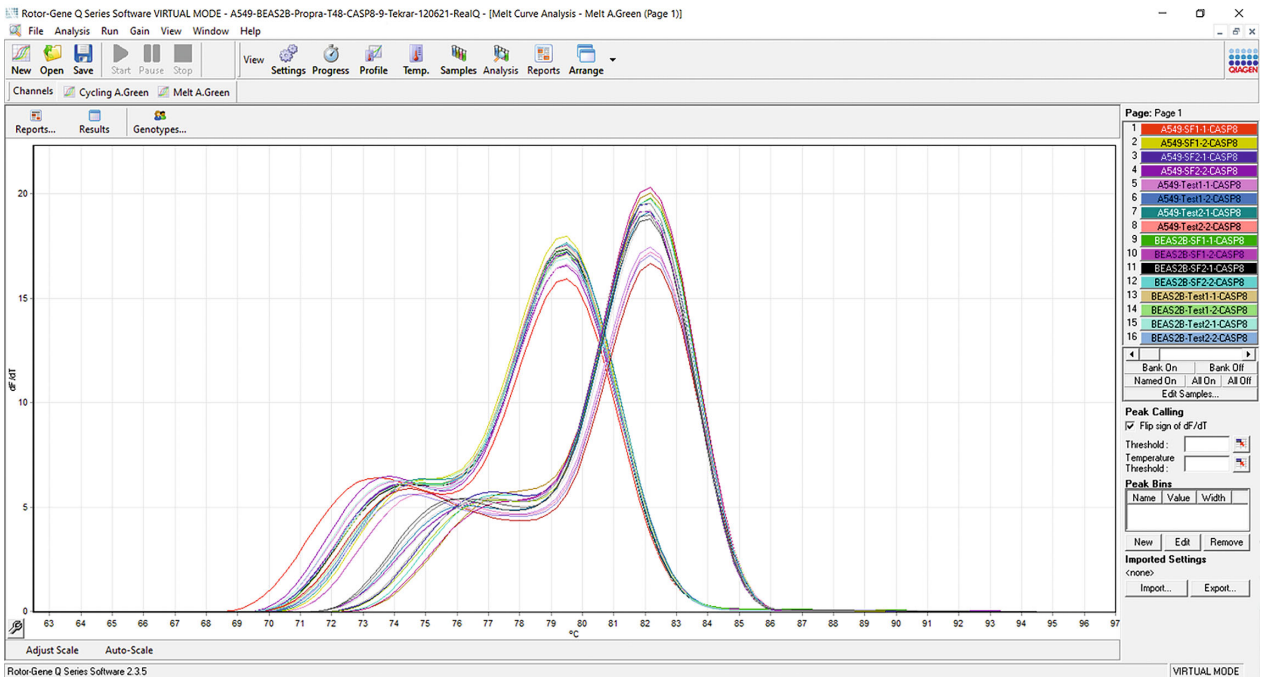
Lung cancer is one of the most prevalent cancer type worldwide along with more than 1.7 million of deaths annually among cancer-related mortalities (1–3). The prognosis of lung cancer is still not at the desired point despite the advanced therapeutic strategies such as tumorectomy, chemo-/radio-therapy, immune therapy, etc. (4). In this regard, developing alternative or corroborative therapy strategies is of vital importance to reduce side effects of conventional cancer therapies and to overcome the resistance of cancer cells (4, 5). Cancer patients experience highly distressed mood as a part of diagnostic and therapeutic period. Several studies have reported that chronic stress and psychosocial factors are correlated with cancer risk and chronic stress hormones are claimed to sustain tumor progression (6–8). Of which, norepinephrine and epinephrine exert their biological effects via α 1-, α 2-, and β -adrenergic receptors (β -ARs) that transmit signals through various biochemical pathways in several tissues (9–11). Preclinical studies have reported that stress hormones mediate their direct effects on tumor cells through mostly G protein-coupled β -ARs (GPCRs) (2, 12, 13). β -adrenergic signaling pathway has been previously demonstrated to be implicated also in tumorigenesis of several cancer types via modulation of certain pathways including DNA repair and apoptosis (5). Similar studies also revealed that β -adrenergic receptor antagonists, so called β -blockers, exerted potential beneficial effects as an adjuvant therapeutic option in the treatment of cancers by inhibiting metastasis, tissue invasion, and angiogenesis via blocking VEGF and IL-6 (5, 13, 14).

Propranolol (PRO) is a non-selective β -AR antagonist commonly used as prophylaxis in the treatment of hypertension, angina, anxiety, cardiac arrhythmia, hyperthyroidism, essential tremor and migraine, variceal bleeding, and myocardial infarction (7, 15, 16). The research about the anti-tumorigenic effects of PRO have been commenced with the studies investigating basically the role of catecholamines in carcinogenesis and their affinities to the various binding sites of β -ARs in several tissues (7). Especially, coincidental observations with respect to the therapeutic effects of PRO on hemangiomas have revived the attention on the discoveries regarding its anti-angiogenic and anti-tumorigenic activities

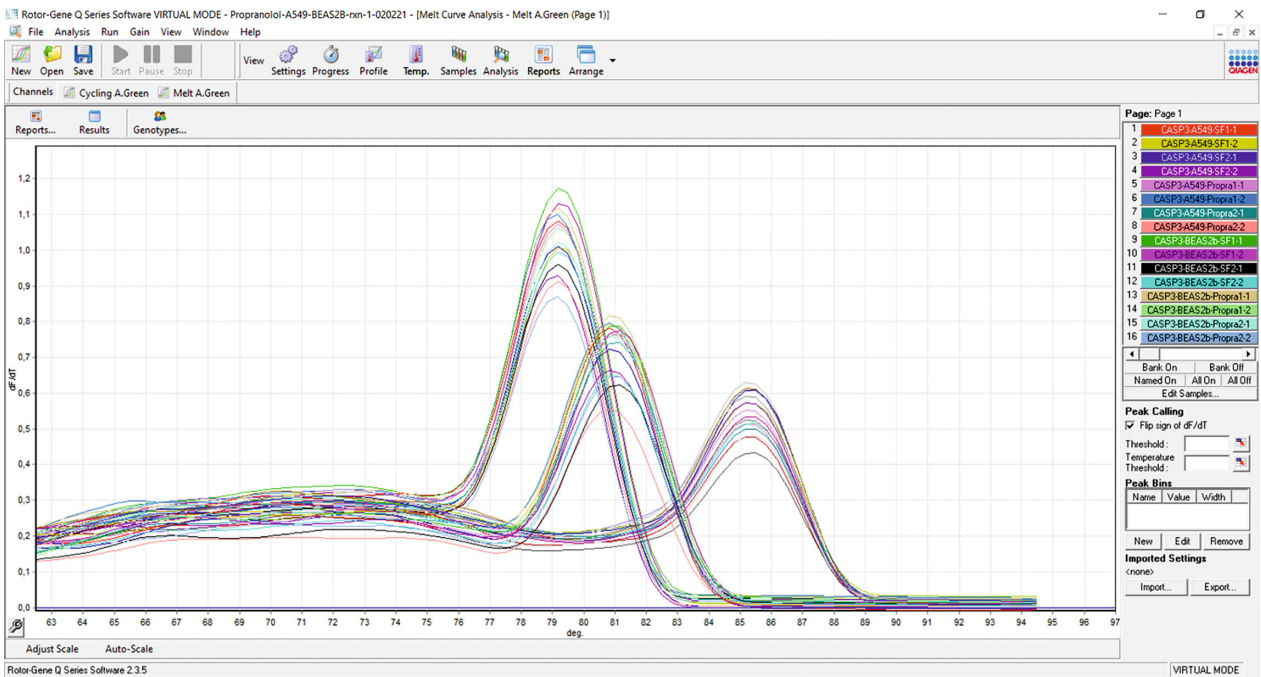
Propranolol (PRO) is a non-selective β -AR antagonist commonly used as prophylaxis in the treatment of hypertension, angina, anxiety, cardiac arrhythmia, hyperthyroidism, essential tremor and migraine, variceal bleeding, and myocardial infarction (7, 15, 16). The research about the anti-tumorigenic effects of PRO have been commenced with the studies investigating basically the role of catecholamines in carcinogenesis and their affinities to the various binding sites of β -ARs in several tissues (7). Especially, coincidental observations with respect to the therapeutic effects of PRO on hemangiomas have revived the attention on the discoveries regarding its anti-angiogenic and anti-tumorigenic activities

¹Department of Medical Biology, Faculty of Medicine, Hatay Mustafa Kemal University, Hatay, Turkey, and ²Department of Molecular Biochemistry and Genetics, Graduate School of Health Sciences, Hatay Mustafa Kemal University, Hatay, Turkey

Address for correspondence: Menderes Yusuf TERZI, Assoc Prof, PhD, Hatay Mustafa Kemal University Faculty of Medicine Department of Medical Biology, Tayfur Ata Sökmen Campus, 31060, Antakya-Hatay, Turkey. Phone: +90.530.7225632



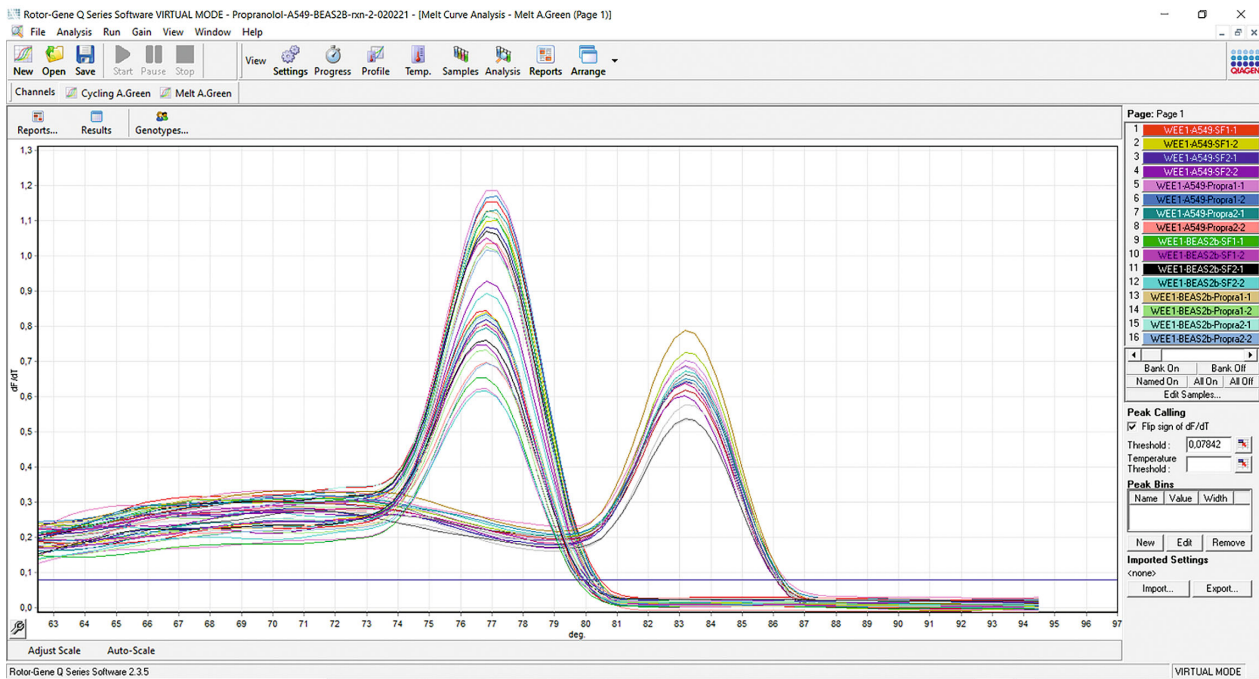
Supplementary Fig. 1. Representative melting curves of target genes; CASP8 and CASP9 in A549 and BEAS2B cells analyzed with qPCR.



Supplementary Fig. 2. Representative melting curves of target genes; CASP3, CDKN1A, GAPDH in A549 and BEAS2B cells analyzed with qPCR.

(17). So that PRO can be a promising adjuvant agent against the lung cancer progression. In this context, we aimed in this study to investigate the *in vitro* effects of PRO on cell viability, apoptosis, and cell cycle in A549 lung cancer cells and healthy lung epithelial cells BEAS2B. For this purpose, prominent apoptosis-related proteins; caspases (3, 8, and 9), apoptosis inducing factor (AIF),

and DNA damage inducible transcript 3 (DDIT3) and cell cycle regulatory proteins; WEE1 G2 checkpoint kinase (WEE1) and cyclin dependent kinase inhibitor 1A (CDKN1A) were selected to analyze the effect of PRO on both, lung cancer and healthy lung cells (18, 19).



Supplementary Fig. 3. Representative melting curves of target genes; WEE1, DDIT3, AIF1 in A549 and BEAS2B cells analyzed with qPCR.

Material and methods

Culture of A549 and BEAS2B cell lines

A549 human lung adenocarcinoma and its non-syngeneic form; non-tumorigenic BEAS2B human lung bronchial epithelial cell lines, previously purchased from American Type Culture Collection, were obtained from cell culture stocks of Department of Medical Biology, Hatay Mustafa Kemal University. We cultured the cells with Dulbecco's Modified Eagle Medium (DMEM, Gibco) containing 1 % L-glutamine, 10 % fetal bovine serum (FBS, Hyclone), and 1 % penicillin/streptomycin (Hyclone) medium in T75 cell culture flasks (Corning). The cells were incubated under 37 °C and 5 % CO₂ conditions for proliferation. We passaged the cells after they reached 70–80 % confluency and replaced the cell media with fresh one at every 2–3 days.

Cell viability assay

We measured the effect of PRO on the cell viability of A549 and BEAS2B cells based on the 3-(4,5-Dimethylthiazol-2-yl)-2,5-diphenyltetrazolium bromide (MTT) assay. Hence, we seeded 96-well cell culture plates with 10⁴ cells per mL (100 µl/well). After cells reached confluency, we treated the cells in the test group with 0 (zero), 7.81, 15.63, 31.25, 62.50, 125, 250, and 500 µM PRO in serum-free cell medium for 24 h in 37 °C incubator. Then the media were replaced with 1 mg/mL MTT (100 µl) (Sigma Aldrich, USA) in DPBS (Sigma Aldrich, Germany) to incubate for ~ 2–3 hours at 37 °C. Thereafter, MTT solution was removed, and the cells were treated with 100 µl DMSO solution for another 5 min at room temperature (RT) with gentle shaking. The plate was put

into a spectrophotometer (Multiskan Go, Thermo Fisher, Finland) to analyze color spectrum change at 590 nm and 670 nm as the reference wavelength. We expressed the cell viability as the percentage of control group and calculated the half-maximal inhibitory concentration (IC₅₀) values for each cell line by using the best fit curve analysis in GraphPad prism.

Colony formation assay

Colony formation assay was performed on A549 cells to analyze the effect of PRO on the clonogenic efficiency of cancer cells. Colony formation assay was performed as described previously with minor modifications (20). To summarize, 50 cells/mL were seeded into 6-well plate for 10 days of incubation. Then the colonies comprising 10–15 cells were counted with a phase contrast microscope (Nikon Eclipse TS100, Tokyo, Japan) for final analysis. The colony formation efficiency was calculated as the following: number of counted colonies / (number of initial seeded cells) x 100.

Analysis of relative mRNA expression with quantitative reverse transcription-PCR (qRT-PCR)

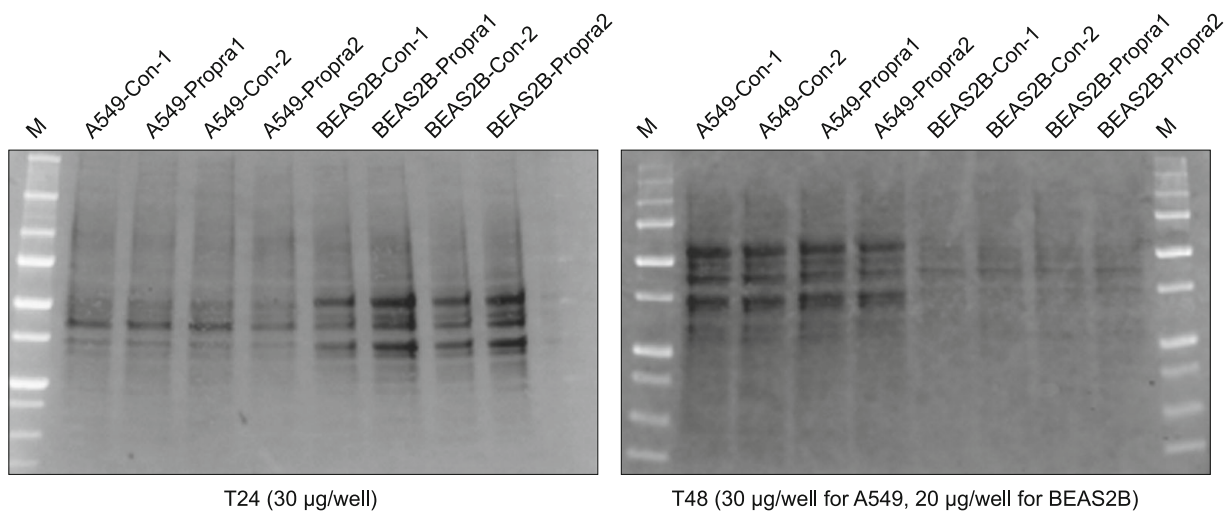
We measured relative gene expression levels of *CDKN1A* (*p21*), *WEE1*, *DDIT3* (*CHOP*), *AIF1*, *CASP3*, *CASP8*, and *CASP9* via qRT-PCR method. Initially, we seeded A549 and BEAS2B cells with a density of 10⁵ cells/mL into 6-well plates for about 24 h to ensure adherence. Then we treated A549 and BEAS2B cells with sub-cytotoxic concentrations of PRO i.e., 100 µM and 125 µM respectively, in serum-free medium for 24 h while control cells received just serum-free medium without PRO. After treatment

Tab. 1. Primers used in qPCR analyses.

Gene symbol	Primer sequence	Amplicon (bp)	Anneal. (°C), Cycle	Ref. Seq.
<i>DDIT3</i>	F: 5'-CTTCTCTGGCTTGGCTGACTGA-3' R: 5'-TGACTGGAATCTGGAGAGTGAGG-3'	88	60,40x	NM_001195053.1
<i>AIF1</i>	F: 5'-GTGCCTATGCCTACAAGACTATG-3' R: 5'-TCTGTTTCTGTCTGGTGTGAG-3'	90	60,40x	NM_004208.4
<i>CDKN1A</i>	F: 5'-CCGAAGTCAGTTCCTTGTGG-3' R: 5'-CATGGGTTCTGACGGACAT-3'	112	60,40x	NM_000389.5
<i>WEE1</i>	F: 5'-ACCACAAGTGCTTCCCAAGA-3' R: 5'-CAGTGCCATTGCTGAAGGTC-3'	88	60,40x	NM_003390.4
<i>CASP3</i>	F: 5'-CTTCTACAACGATCCCCTCTGA-3' R: 5'-TGTGCTTCTGAGCCATGGTG-3'	102	60,40x	NM_004346.4
<i>GAPDH</i>	F: 5'-GTCAACGGATTTGGTCGTATTG-3' R: 5'-TGTAGTTGAGGTCAATGAAGGG-3'	106	60,40x	NM_002046.7
	Gene Globe ID*			
<i>CASP8</i>	PPH00359F	65	60, 40x	
<i>CASP9</i>	PPH00353B	114	60, 40x	

AIF1 – Apoptosis inducing factor mitochondria associated 1, DDIT3 – DNA damage inducible transcript 3, CDKN1A – Cyclin dependent kinase inhibitor 1A, WEE1 – WEE1 G2 checkpoint kinase, CASP3, CASP8, CASP9 – Caspases 3, 8, 9, GAPDH – Glyceraldehyde-3-phosphate dehydrogenase, bp – base pair, F – forward primer sequence, R – reverse primer sequence, Anneal. – Annealing temperature, X – times of cycle, Ref. Seq. – NCBI reference sequence. *Qiagen RT² qPCR Primer Assays (Maryland, USA)

Westernblot total protein loading control (CASP3)



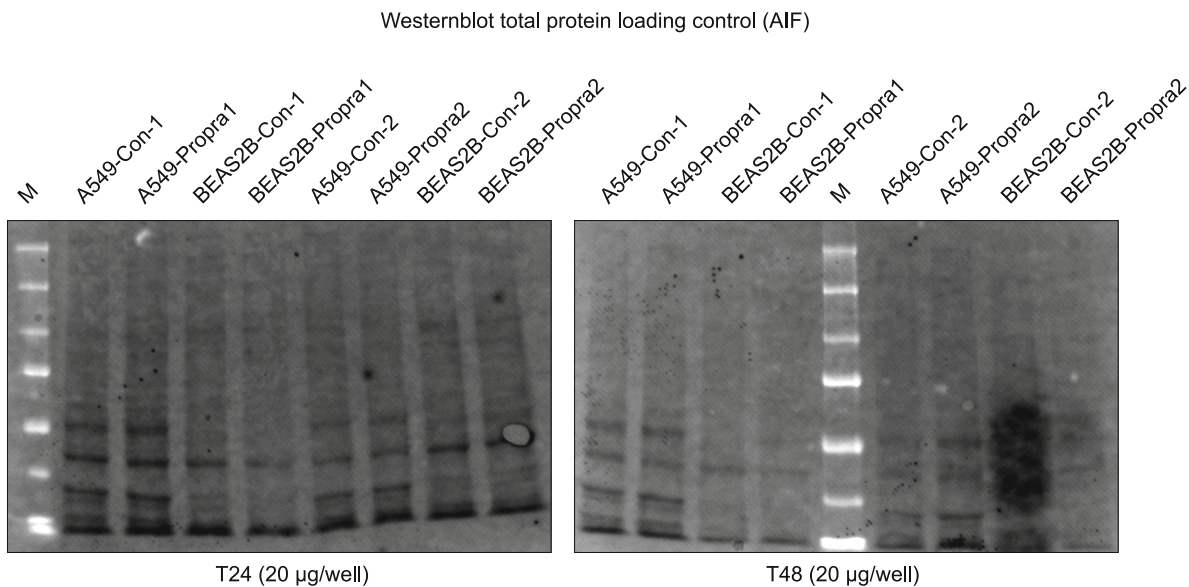
Supplementary Fig. 4. Western blot total protein loading controls for CASP3 analysis at 24 h and 48 h. Bright-white lanes are representing the protein markers on the blot. Each lane consisting of dark black bands represents an individual sample. The amount of total loaded protein; at 24 h for both cell lines is 30 µg/well and at 48 h; 30 µg/well for A549 and 20 µg/well for BEAS2B cells. M: Marker, Con: Control, Propra: Propranolol.

we harvested all cells to isolate total RNA (Gene jet RNA Purification Kit, Thermo Fisher, USA). We diluted all RNA samples after concentration measurements (μ Drop, Thermo Scientific) to get 2 μ g RNA as the final amount for each cDNA conversion reaction (High-Capacity cDNA-RT-Kit, Thermo Scientific) in a thermal cycler (Bio-Rad). We diluted the cDNAs for further real time gene expression analyses in Rotor Gene Q (Qiagen, Hilden, Germany). Sybr green (Maxima SYBR Green, Thermo Fisher Scientific, Lithuania) detection method was utilized with the following reaction steps: 2 min at 50 °C, 10 min at 95 °C, 40 cycles: [15 sec at 95 °C, 1 min at 60 °C]. Melting curve analyses were performed at the end of each qPCR reaction to confirm the ampli-

con size of the target genes and primer specificity (Supplementary Figs 1–3). We normalized the Ct values of target genes by using glyceraldehyde-3-phosphate dehydrogenase (*GAPDH*). We used Livak method ($2^{-\Delta\Delta Ct}$) to express the relative mRNA levels of the target genes as fold change (21). We listed the designed primer sequences (Thermo Fisher Scientific, Lithuania) of the corresponding target genes used in real time PCR in Table 1.

Total protein isolation and quantification

The cells were seeded into 6-well plates at a ratio of 10^5 cells/well. After the cells reached confluence, sub-cytotoxic concentrations of PRO were added into the culture medium and incubated for



Supplementary Fig. 5. Western blot total protein loading controls for AIF analysis at 24 h and 48 h. Bright-white lanes are representing the protein markers on the blot. Each lane consisting of dark black bands represents an individual sample. The amount of total loaded protein is 20 µg/well for each time point and cell line. M: Marker, Con: Control, Propra: Propranolol.

24-h in CO₂ incubator. After that, the cells were rinsed with ice-cold DPBS (Thermo Scientific) once and incubated in RIPA buffer containing protease inhibitor cocktail (Thermo Scientific) for 15 min on ice with gentle shaking. Then cell lysate was collected with a cell scraper and centrifuged at 13000xg for 5 min and supernatants were transferred into microfuge tubes in several aliquots and kept at –20 °C. All protein samples were quantified with BCA assay (Thermo Scientific). Total protein concentrations were calculated to equalize the protein amount for the following Western blot analysis.

Western blot protein analysis

In order to analyze protein expression levels of total and cleaved CASP3, 20–30 µg protein/well was loaded into SDS-PAGE ready-to-use stain-free gels (Bio-Rad). After running of proteins under constant 200 V current for about 20–30 min. (Bio-Rad), the blotting was performed using PVDF membrane for about 3–7 min using turbo-blot transfer settings of semi-dry blotting system (Bio-Rad). After imaging total protein on both the gel and the membrane to evaluate transfer efficiency, the blot was washed with TBS-T and incubated in a commercial blocking solution (Thermo Scientific) for 1 h at RT. After washing, the blot was incubated with primary rabbit anti-CASP3 (Cell Signaling Technology) and rabbit anti-AIF (Cell Signaling Technology) antibodies overnight at 4 °C on a shaker. The blot was washed several times and incubated with secondary HRP-conjugated anti-rabbit antibody for 1 h at RT. After final washing step, the blot was re-imaged to visualize total protein bands per well in order to normalize the band signals of target proteins (Supplementary Figs 4–5). Thereafter, the blot was exposed to the HRP substrate (Bio-Rad) for about 10–15 min.

Finally, the blot was imaged under chemiluminescence channel to visualize target specific bands. All imaging and analyses were performed with ChemiDoc Image Analyzer (Bio-Rad).

Statistical analysis

The Gaussian distribution of whole data was analyzed with Shapiro Wilk's normalization test. The data of multiple groups were analyzed with one-way ANOVA or Kruskal Wallis tests and the comparison between two individual groups were performed with Dunnett's multiple comparison test. The comparison of control and test groups were performed with two-way unpaired student's t-test or Mann-Whitney U tests. The experiments were performed at least in triplicates. All data were expressed as mean ± SEM or mean ± SD. Statistically, the p values less than 0.05 were accepted as significant. The GraphPad Prism software version 8.0.2 (263) was used to prepare plots and for all statistical analyses.

Results

Reduced cell viability after PRO treatment

We tested the effect of several PRO concentrations on the cell viability of A549 and BEAS2B cells. As depicted in Figure 1, PRO, at several concentrations, significantly lowered the cell viability of both cancer and non-cancer cell lines after 24 h ($p < 0.05$). However, both microscopic (Fig. 1A) and spectroscopic (Fig. 1B) analyses revealed that PRO exerted higher cellular toxicity on A549 cells compared to BEAS2B cells since IC₅₀ values were calculated as 147.7 µM and 159.6 µM, respectively. Moreover, BEAS2B cells were more resistant to PRO's lower concen-

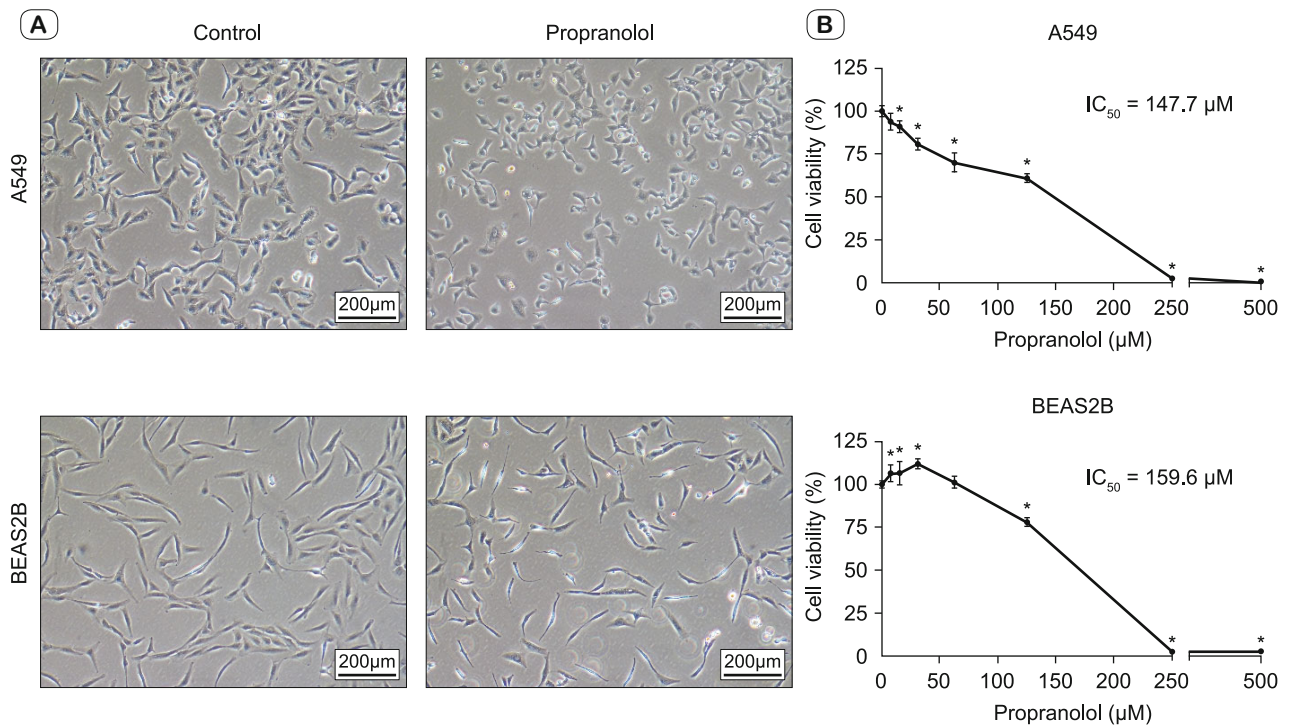


Fig. 1. Representative microscopic photos after treatment with non-cytotoxic concentration of propranolol for 24 h (A) and MTT analysis to test cell viability after treatment with 0 (zero), 7.81, 15.63, 31.25, 62.50, 125, 250, and 500 µM propranolol in A549 and BEAS2B cells for 24 h (B). Cell viability was expressed as the percentage (%) of control cells (Control cells were treated with serum-free medium without propranolol). IC_{50} values were calculated with GraphPad prism. Data were expressed as mean \pm SD (n = 5). * p < 0.05. Scale bars = 200 µm.

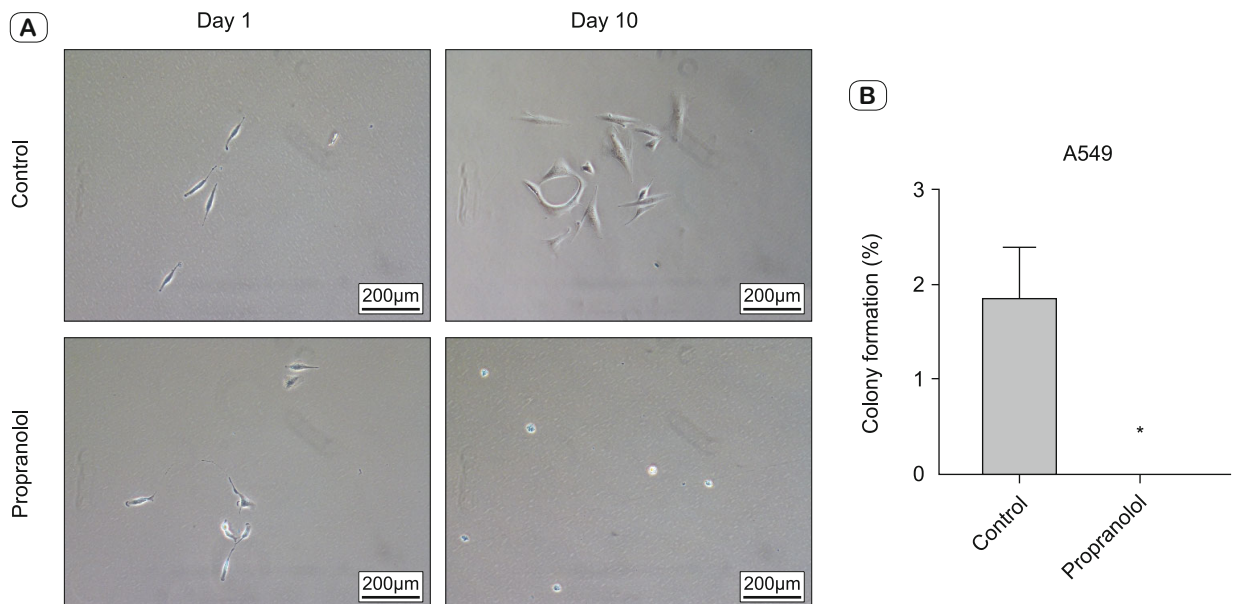


Fig. 2. Representative microscopic photos of colony formation assay after treatment with non-cytotoxic concentration of propranolol for 10 days (A) and the analysis of colony formation efficiency in A549 cells (B). Colony formation was calculated as the percentage (%) of colonies based on the initially seeded cell number. Data were expressed as mean \pm SEM (n = 3). * p < 0.05. Scale bars = 200 µm.

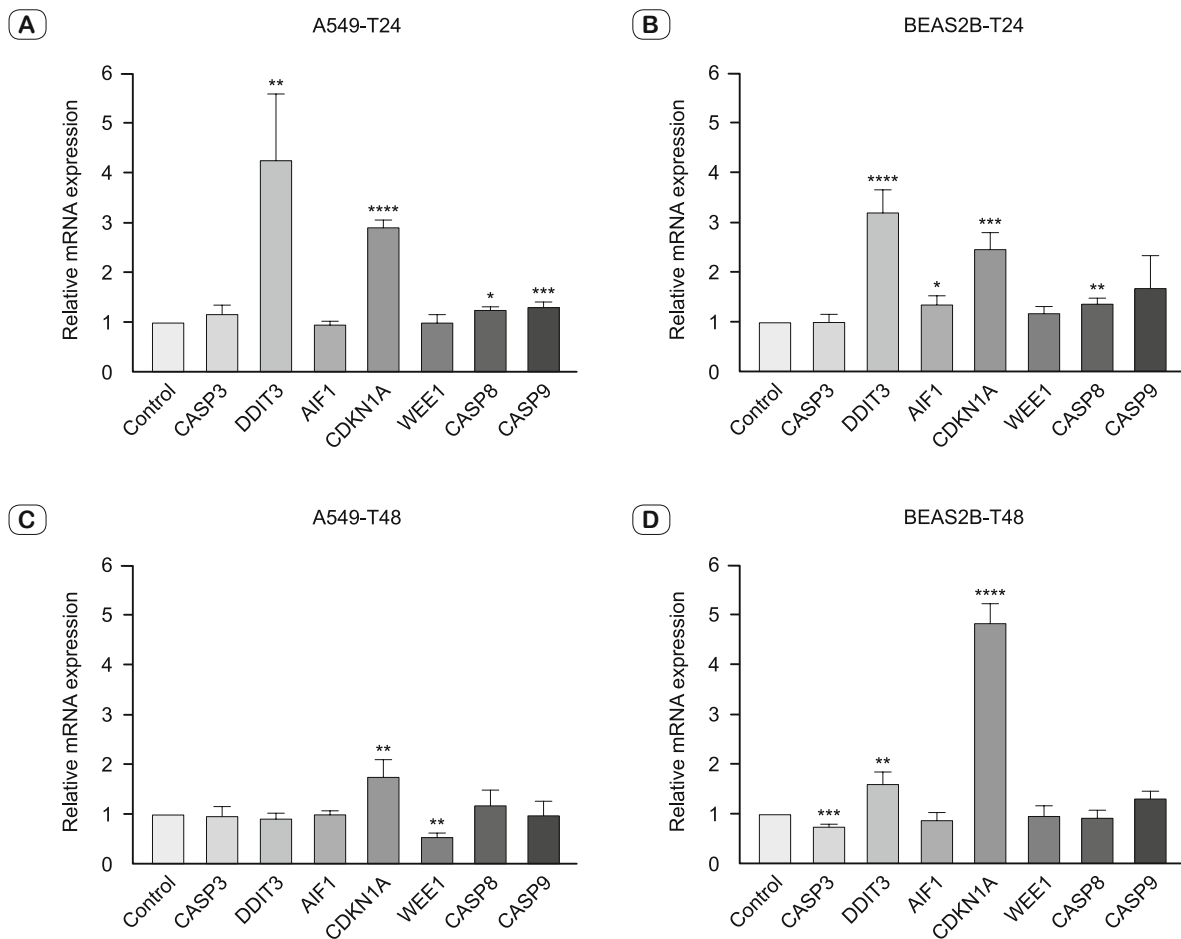


Fig. 3. Relative mRNA levels of CASP3, DDIT3, AIF1, CDKN1A, WEE1, CASP8, and CASP9; after propranolol treatment at 24 h in A549 (A) and BEAS2B cells (B) and at 48 h in A549 (C) and BEAS2B cells (D). Gene expression levels were expressed as the fold change ($2^{-\Delta\Delta Ct}$) of control group. Data were expressed as mean \pm SEM (n = 4). * p < 0.05, ** p < 0.001, *** p < 0.0005, **** p < 0.0001. Glyceraldehyde-3-phosphate dehydrogenase gene was used for the normalization. AIF1: Apoptosis inducing factor mitochondria associated 1, DDIT3: DNA damage inducible transcript 3, CDKN1A: Cyclin dependent kinase inhibitor 1A, WEE1: WEE1 G2 checkpoint kinase, CASP3, CASP8, CASP9: Caspases 3, 8, 9.

treatments compared to A549 cells; although the cell loss was 30 % in A549 cells at 62.5 μ M PRO concentration, no cell loss was observed in BEAS2B cells at the same concentration (Fig. 1B). To conduct further analyses, we picked the sub-cytotoxic concentrations of PRO as 100 μ M and 125 μ M for A549 and BEAS2B, respectively.

PRO diminished A549 colonies post-treatment

The clonogenic efficiency of A549 cells for 10 days post-PRO treatment was analyzed under phase contrast microscope. The microscopic evaluation (Fig. 2A) showed that 100 μ M PRO treatment completely diminished the A549 colonies after 10 days of incubation (Fig. 2B) (p < 0.05).

Cell cycle arrest of both cell types via different pathways

The gene expression levels of cell cycle regulatory proteins, WEE1 and CDKN1A (p21), were analyzed with qRT-PCR after

24 h and 48 h PRO treatments in A549 and BEAS2B cells. We found that *CDKN1A* expression significantly increased in both cell lines at both time points (Fig. 3) (p < 0.05). On the other hand, *WEE1* showed a spatiotemporal expression pattern meaning; its levels did not change after PRO treatment at any time points in BEAS2B cells (Figs 3B, D) (p > 0.05) while decreased in A549 cells after 48 h of PRO treatment (Fig. 3C) (p < 0.05) with steady levels after 24 h (Fig. 3A) (p > 0.05).

Altered gene expression patterns of apoptosis-related genes in A549 and BEAS2B cells

We measured the mRNA levels of apoptosis-related genes after PRO treatment in A549 and BEAS2B cells. *CASP3* expression did not change in A549 cells at either time point (Figs 3A, C, p > 0.05) while *CASP8* and *CASP9* significantly increased after 24 h PRO treatment (Fig. 3A) (p < 0.05) with steady levels at 48 h (Fig. 3C) (p > 0.05). In BEAS2B cells, PRO altered the expres-

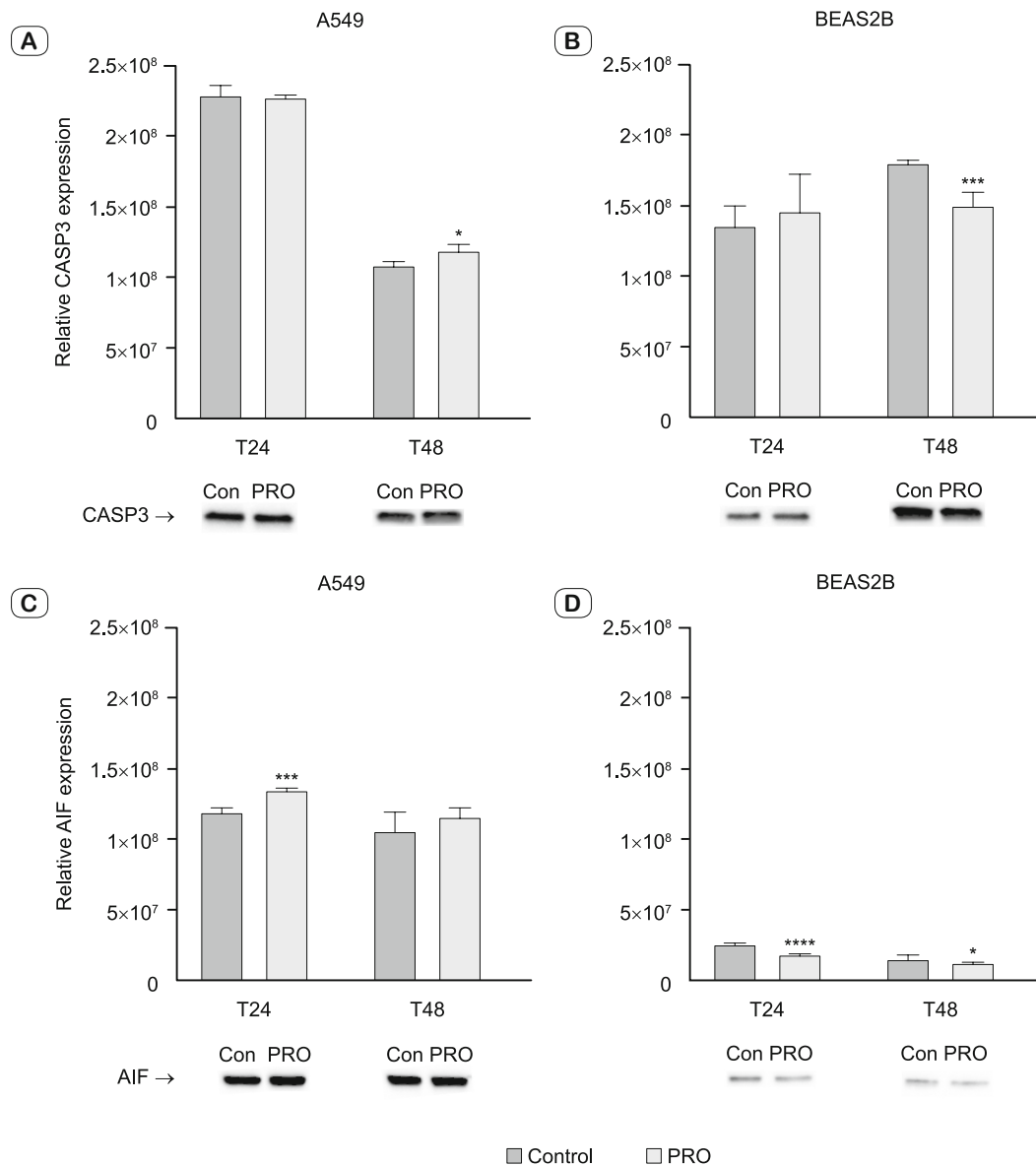


Fig. 4. Relative protein expression levels analyzed with Western blot. Effect of propranolol treatment; on CASP3 protein levels at 24 h and 48 h in A549 (A) and BEAS2B cells (B), and on AIF1 levels at 48 h in A549 (C) and BEAS2B cells (D). Protein expression levels were normalized based on the total protein loaded. Data were expressed as mean \pm SD (n = 4). * p < 0.05, ** p < 0.001, *** p < 0.0005, **** p < 0.0001. CASP3: Caspases 3, AIF1: Apoptosis inducing factor mitochondria associated 1.

sion of CASP8 just at 24h with an upregulation and the expression of CASP3 at 48 h with a downregulation (Figs 3B, D) (p < 0.05). The CASP9 expression did not show any significant change at any time points (Figs 3B, D) (p > 0.05). Regarding other apoptotic markers, PRO treatment significantly upregulated DDIT3 expression at all time points in BEAS2B cells and at 24 h in A549 cells (Figs 3A, B, and D) (p < 0.05) but returned to steady levels in A549 cells at 48 h (Fig. 3C) (p > 0.05). Moreover, PRO significantly elevated the mRNA levels of AIF1 at 24 h in BEAS2B cells (Fig. 3B) (p < 0.05) but did not cause any significant change

at other time points in A549 and BEAS2B cells (Figs 3A, C, and D) (p > 0.05).

Reverse effects of PRO on protein levels of apoptotic CASP3 and AIF1 in cancer and healthy cells

We sought to analyze the protein levels of the main mediators and executioners of caspase-dependent (CASP3) and caspase-independent (AIF1) apoptotic pathways after PRO treatment in A549 and BEAS2B cells with Western blot. We have shown that, PRO treatment significantly increased the CASP3 protein levels

after 48 h in A549 cells (Fig. 4A) ($p < 0.05$) although it did not show any effect at 24 h (Fig. 4A) ($p > 0.05$). On the contrary, the CASP3 protein levels significantly decreased in BEAS2B cells 48 h post PRO treatment (Fig. 4B) ($p < 0.05$), but remained unchanged at 24 h (Fig. 4B) ($p > 0.05$). A similar pattern to CASP3 protein expression was observed in AIF1 levels in A549 and BEAS2B cells. AIF1 upregulated at 24 h in A549 cells and returned to its basal levels at 48 h in A549 cells (Fig. 4C). In BEAS2B, PRO significantly reduced the AIF1 protein levels at both time points (Fig. 4D) ($p < 0.05$). We also tried to measure the protein levels of DDIT3, as a prominent endoplasmic stress-induced apoptotic marker, but we found no detectable signal after Western blot analysis (data not shown).

Discussion

In the current study, we analyzed the effect of a non-selective β -blocker called PRO, a commonly used drug against hypertension, on the cell viability and the regulatory proteins involved in both apoptosis and cell cycle control in human epithelial lung cancer cell line A549 and its nonsyngeneic and nontumorigenic form of human bronchial cell line BEAS2B with qRT-PCR and Western blot analyses. Apart from previous studies in the literature, we demonstrated that cytotoxicity of PRO was higher in A549 cells compared to BEAS2B cells. Besides, our data revealed that PRO-induced cell death in A549 cells was mediated via both, caspase-dependent (CASP3, 8, 9) and independent (AIF1) pathways. On the other hand, the reduced cell viability in BEAS2B cells was most likely caused by the sustained cell cycle inhibition via increased levels of CDKN1A due to reduced protein levels of cells death markers i.e., CASP3 and AIF1. Given that the discovery of novel anti-cancer drugs is costly and a time-consuming procedure, developing alternative treatment strategies, e.g. the reuse of established drugs against other diseases in a combinatory way, is less costly and can yield unexpected promising outcomes within shorter time period (4). Of which, PRO, a commonly used β -AR antagonist in cardiac and hypertensive patients, has been shown to be anti-tumorigenic owing to its inhibitory effects on tumor progression by blocking β -ARs whose expression is upregulated in several tumor types such as mammary, colon, and pancreas cancers (7, 22, 23). Moreover, in vitro and clinical studies have claimed that PRO could corroborate the treatment efficiency by increasing the conventional treatment of human cancer cells in a combinatory manner (17, 24–26).

In our study, several concentrations of PRO have significantly reduced cell viability in both A549 cancer cells and nontumoral BEAS2B lung cells. We observed after cell viability analysis that cytotoxicity of PRO in A549 cells was higher compared to BEAS2B cells. Furthermore, the colony-forming efficiency of A549 cells has diminished after 10-day long 100 μ M PRO exposure. β -adrenergic agents are known as strong mitogenic agents (22). In a study conducted with different cancer cell lines, even low PRO concentration as 25 μ M has led to reduction in cell proliferation at a ratio between 15 % to 67 % depending on the

cancer type (27). In another in vitro study with pancreatic cancer cells, PRO caused maximum response at 100 μ M concentration regarding the inhibition of cell proliferation (28).

Our gene expression data revealed that treatment of A549 and BEAS2B cells with PRO for 24 h and 48 h led to significant increase in the mRNA levels of *CDKN1A* at both time points and cell types. We also found that *WEE1*, another prominent cell cycle regulatory gene, remained at basal level after 24h post-PRO treatment in A549 cells but decreased after 48h. However, in non-tumoral BEAS2B cells, *WEE1* gene expression did not show a significant change. In a previous in vitro study designed to enlighten the inhibitory action mechanism of PRO against proliferation of SVR vascular tumor cells, it was reported that 24h-long 100 μ M PRO treatment upregulated the mRNA levels of *CDKN1A* 4.7-times and *WEE1* 1.2-times (27). It is known that under unfavorable conditions p53-induced *CDKN1A* arrests cell cycle especially at G1 and G2 check points by interfering with cyclin-dependent kinases while *WEE1* is mostly active at S phase (29-31). *WEE1* arrests the dividing cells at G2/M phase check point if a DNA damage response is present (32). Previous studies showed that inhibition of *WEE1* expression in several breast cancer cell lines drove the cells at S-phase or G2-phase directly into M phase without check point regulations, which eventually drives tumor cells into apoptosis due to accumulated mutations caused by premature mitosis (33–36). Our gene expression data i.e., reduced *WEE1* levels in tumor cells post-PRO treatment, are in line with these findings. On the other hand, the steady levels of *WEE1* post-PRO treatment in nontumoral BEAS2B cells can be interpreted as a resistance or survival struggle of cells against apoptosis. In this context, the versatile expression levels and patterns of cell cycle regulatory proteins in our study could arise from the triggering of different decision mechanisms regarding cell fate depending on the tumorigenicity of the cell types.

Apoptosis is a vital mechanism during embryogenesis as well as a defense mechanism against infections and tumorigenesis (18). Especially caspase enzymes are the main initiators and executioners of the apoptosis. There are also caspase-independent pathways in the cells promoted by mitochondrial nucleases such as AIF1 and endonuclease G proteins (37, 38). It has been known that disruption of apoptosis via mutations in apoptosis-related players such as p53, or *BCL2* result in tumorigenesis and metastasis (18). Vice versa, as a cancer therapeutic strategy, the induction of apoptosis is an effective strategy in eradication of tumor cells (18, 39). In a mouse model of ovarian cancer, it was shown that PRO treatment reversed the β -adrenergic activation-induced tumor angiogenesis by blocking cAMP–PKA signaling pathway (40). PRO exerts its anti-tumorigenic effects not only by blocking angiogenesis but also through triggering apoptosis, suppressing anti-apoptotic mediators, and inhibiting proliferation and invasion/metastasis of tumor cells (41, 42).

In this regard, we checked the effect of PRO on mRNA levels of *CASP 3*, 8, and 9, and as caspase-independent apoptotic players *AIF* and *DDIT3* genes in both tumoral and nontumoral cells. We also measured the protein levels of CASP3 and AIF1 with western

blot to observe apoptotic effect of PRO on A549 tumor and BEAS2B non-tumoral lung cells. We found that, while the mRNA levels of *CASP 8* and *9* in A549 cell increased significantly 24h post-PRO treatment, *CASP3* gene expression did not exhibit any significant alteration. However, *CASP3* protein level increased after 48h suggesting that the initiator caspases i.e., *CASP8* and *9*, induced both intrinsic and extrinsic apoptotic pathways which resulted in upregulation of effector *CASP3* in tumor cells. An *in vitro* study with pancreatic cancer cell line demonstrated that PRO could inhibit cell proliferation by triggering apoptosis via only mitochondrial caspase-dependent pathway (41). In another study conducted with human ovarian cell line, PRO induced both intrinsic and extrinsic pathways (15). In line with these studies, we demonstrated that PRO triggered caspase-dependent apoptotic pathway in lung tumor cells.

As to BEAS2B cells, just *CASP8*, as initiator caspase of extrinsic pathway, significantly increased at 24 h but it returned to basal levels at 48 h. More strikingly, *CASP3* gene expression significantly dropped down in BEAS2B cells 48 h post-PRO treatment. In line with the mRNA expression data, protein levels of *CASP3* also significantly decreased in BEAS2B cells after 48 h PRO treatment. Contrary to tumoral A549 cells, the reversal of early apoptotic induction in BEAS2B cells after cell cycle arrest mediated by *CDKN1A* indicates that PRO exerted its apoptotic action based on cell type and exposure duration. Our data corresponding to apoptotic markers were also in parallel with the spatiotemporal expression pattern of cell cycle regulatory gene *WEE1* as aforementioned above.

The fact that some cancer types may lack *CASP3* expression due to the gene deletion or blockage of caspase pathways makes the apoptosis-inducing agents find alternative caspase-independent pathways like AIF-promoted cell death (43, 44). In the current study we also focused on AIF1 as an upstream apoptotic player involved in caspase-independent pathway. In the present study, we demonstrated the elevated protein level of AIF after 24h PRO treatment in A549 cells. We know from previous studies that AIF can also be induced coordinately with the caspase-dependent pathway to complement apoptosis (45). Induction of AIF also in our lung cancer model, as an alternative caspase-independent apoptotic molecule, could be upregulated as a back-up pathway to support caspase-mediated apoptosis. On the other hand, we observed that AIF protein expression was downregulated at both time points in BEAS2B cells despite the increased mRNA level at 24h post-PRO treatment. So, it may be claimed from our data that the apoptosis triggered by PRO is depended on the tumorigenicity of the target cells.

Emerging evidence clearly indicates that there are multiple alternative pathways that lead the tumor cells to apoptosis (46). *DDIT3* (CHOP) is a transcription factor which controls proliferation, differentiation, and apoptosis of the cells. It was shown in several cancer cell lines that *DDIT3* acted as a pro-apoptotic factor under oxidative stress by activating effector caspases and inhibiting *BCL2* via endoplasmic reticulum (47, 48). We also checked the mRNA levels of *DDIT3* to analyze alternative apoptotic signals after PRO treatment in our tumoral and nontumoral

cell lines. A previous *in vitro* model with angiosarcoma cells reported that after a global gene expression analysis comprising 428 genes, *DDIT3* gene expression remained unchanged after PRO treatment (27). It has been previously suggested that *DDIT3*, the central regulator of ER stress-induced apoptosis, played role in the regulation of cell cycle regulatory protein *CDKN1A* (49). Moreover, it was stated that elevated *CDKN1A* levels induced the cell cycle arrest and sustained the cell survival signal in the early phase of ER stress response in tumor cells by inhibiting apoptosis after unfolded protein response (49). *DDIT3* gene expression is at quite low level under normal conditions but increases with the stress signals (50). Along with this, we found in the current study that *DDIT3* mRNA levels significantly increased in both cell lines after 24h-treatment with PRO. After 48h PRO treatment, in tumoral A549 cells *DDIT3* returned to basal levels while it remained as significantly high in non-tumoral BEAS2B cells compared to control group. In line with an *in vitro* study, the significant upregulation of *CDKN1A* from 2.5-fold at 24h to 4.9-fold at 48h via the sustained high levels of *DDIT3* could presumably favor the cell survival pathway over apoptosis in non-tumoral BEAS2B cells unlike tumoral A549 cells in which relative reduction of *DDIT3* and *CDKN1A* triggered apoptotic pathways (49).

Overall, we demonstrated that PRO could reduce cell viability by inducing both caspase-dependent and independent apoptosis in A549 lung tumor cells via *CASP3* and AIF1. In nontumoral BEAS2B lung cells, cell proliferation was blocked through cell cycle regulatory gene *CDKN1A* after PRO treatment. We also suggest that *DDIT3* gene expression pattern together with *CDKN1A* plays a central role in decision of cell fate; particularly in the favor of survival in nontumoral cells and of apoptosis in tumor cells. The anti-tumorigenic effects of PRO on lung tumor cells along with less cytotoxicity in nontumoral lung cells make it a promising safe adjuvant therapeutic agent in cancer treatment.

References

1. Lei Z, Yang W, Zuo Y. Beta-blocker and survival in patients with lung cancer: A meta-analysis. *PLoS One* 2021; 16 (2): e0245773.
2. Nilsson MB, Le X, Heymach JV. beta-Adrenergic Signaling in Lung Cancer: A Potential Role for Beta-Blockers. *J Neuroimmune Pharmacol* 2020; 15 (1): 27–36.
3. Udumyan R, Montgomery S, Fang F, Valdimarsdottir U, Hardardottir H, Ekblom A et al. Beta-Blocker Use and Lung Cancer Mortality in a Nationwide Cohort Study of Patients with Primary Non-Small Cell Lung Cancer. *Cancer Epidemiol Biomarkers Prev* 2020; 29 (1): 119–126.
4. Carlos-Escalante JA, de Jesus-Sanchez M, Rivas-Castro A, Pichardo-Rojas PS, Arce C, Wegman-Ostrosky T. The Use of Antihypertensive Drugs as Coadjuvant Therapy in Cancer. *Front Oncol* 2021; 11: 660943.
5. Cole SW, Sood AK. Molecular pathways: beta-adrenergic signaling in cancer. *Clin Cancer Res* 2012; 18 (5): 1201–1206.

6. Hasegawa H, Saiki I. Psychosocial stress augments tumor development through beta-adrenergic activation in mice. *Jpn J Cancer Res* 2002; 93 (7): 729–735.
7. Pantziarka P, Bouche G, Sukhatme V, Meheus L, Rooman I, Sukhatme VP. Repurposing Drugs in Oncology (ReDO)-Propranolol as an anti-cancer agent. *Ecancelmedscience* 2016; 10: 680.
8. Penninx BW, Guralnik JM, Pahor M, Ferrucci L, Cerhan JR, Wallace RB et al. Chronically depressed mood and cancer risk in older persons. *J Natl Cancer Inst* 1998; 90 (24): 1888–1893.
9. Daly CJ, McGrath JC. Previously unsuspected widespread cellular and tissue distribution of beta-adrenoceptors and its relevance to drug action. *Trends Pharmacol Sci* 2011; 32 (4): 219–226.
10. Oh MS, Guzner A, Wainwright DA, Mohindra NA, Chae YK, Behdad A et al. The Impact of Beta Blockers on Survival Outcomes in Patients With Non-small-cell Lung Cancer Treated With Immune Checkpoint Inhibitors. *Clin Lung Cancer* 2021; 22 (1): e57–e62.
11. Iseri OD, Sahin FI, Terzi YK, Yurtcu E, Erdem SR, Sarialioglu F. beta-Adrenoreceptor antagonists reduce cancer cell proliferation, invasion, and migration. *Pharm Biol* 2014; 52 (11): 1374–1381.
12. Chang PY, Huang WY, Lin CL, Huang TC, Wu YY, Chen JH et al. Propranolol Reduces Cancer Risk: A Population-Based Cohort Study. *Medicine (Baltimore)* 2015; 94 (27): e1097.
13. Montoya A, Varela-Ramirez A, Dickerson E, Pasquier E, Torabi A, Aguilera R et al. The beta adrenergic receptor antagonist propranolol alters mitogenic and apoptotic signaling in late stage breast cancer. *Biomed J* 2019; 42 (3): 155–165.
14. Kwon SY, Chun KJ, Kil HK, Jung N, Shin HA, Jang JY et al. beta2-adrenergic receptor expression and the effects of norepinephrine and propranolol on various head and neck cancer subtypes. *Oncol Lett* 2021; 22 (5): 804.
15. Zhao S, Fan S, Shi Y, Ren H, Hong H, Gao X et al. Propranolol induced apoptosis and autophagy via the ROS/JNK signaling pathway in Human Ovarian Cancer. *J Cancer* 2020; 11 (20): 5900–5910.
16. Sidorova M, Petrikaite V. Anticancer Activity of Selective and Non-Selective Beta Adrenoreceptor Blockers against Non-Small Cell Lung Cancer Cell Lines. 2019.
17. Pasquier E, Ciccolini J, Carre M, Giacometti S, Fanciullino R, Pouchy C et al. Propranolol potentiates the anti-angiogenic effects and anti-tumor efficacy of chemotherapy agents: implication in breast cancer treatment. *Oncotarget* 2011; 2 (10): 797–809.
18. Lowe SW, Lin AW. Apoptosis in cancer. *Carcinogenesis* 2000; 21 (3): 485–495.
19. Zheng YZ, Cao ZG, Hu X, Shao ZM. The endoplasmic reticulum stress markers GRP78 and CHOP predict disease-free survival and responsiveness to chemotherapy in breast cancer. *Breast Cancer Res Treat* 2014; 145 (2): 349–358.
20. Roudi R, Madjd Z, Ebrahimi M, Samani FS, Samadikuchakaraei A. CD44 and CD24 cannot act as cancer stem cell markers in human lung adenocarcinoma cell line A549. *Cell Mol Biol Lett* 2014; 19 (1): 23–36.
21. Livak KJ, Schmittgen TD. Analysis of relative gene expression data using real-time quantitative PCR and the 2^{-Delta Delta C (T)} Method. *Methods* 2001; 25 (4): 402–408.
22. Shang ZJ, Liu K, Liang DF. Expression of beta2-adrenergic receptor in oral squamous cell carcinoma. *J Oral Pathol Med* 2009; 38 (4): 371–376.
23. Hicks BM, Murray LJ, Powe DG, Hughes CM, Cardwell CR. beta-Blocker usage and colorectal cancer mortality: a nested case-control study in the UK Clinical Practice Research Datalink cohort. *Ann Oncol* 2013; 24 (12): 3100–3106.
24. Chaudhary KR, Yan SX, Heilbronner SP, Sonett JR, Stoopler MB, Shu C et al. Effects of beta-Adrenergic Antagonists on Chemoradiation Therapy for Locally Advanced Non-Small Cell Lung Cancer. *J Clin Med* 2019; 8 (5).
25. Rico M, Baglioni M, Bondarenko M, Laluce NC, Rozados V, Andre N et al. Metformin and propranolol combination prevents cancer progression and metastasis in different breast cancer models. *Oncotarget* 2017; 8 (2): 2874–2889.
26. Montoya A, Amaya CN, Belmont A, Diab N, Trevino R, Villanueva G et al. Use of non-selective beta-blockers is associated with decreased tumor proliferative indices in early stage breast cancer. *Oncotarget* 2017; 8 (4): 6446–6460.
27. Stiles JM, Amaya C, Rains S, Diaz D, Pham R, Battiste J et al. Targeting of beta adrenergic receptors results in therapeutic efficacy against models of hemangioendothelioma and angiosarcoma. *PLoS One* 2013; 8 (3): e60021.
28. Zhang D, Ma Q, Shen S, Hu H. Inhibition of pancreatic cancer cell proliferation by propranolol occurs through apoptosis induction: the study of beta-adrenoceptor antagonist's anticancer effect in pancreatic cancer cell. *Pancreas* 2009; 38 (1): 94–100.
29. Aktuğ H. Apoptosis and cell cycle. *Ege Journal of Medicine* 2014; 53 (1): 60–64.
30. Dutto I, Tillhon M, Cazzalini O, Stivala LA, Prosperi E. Biology of the cell cycle inhibitor p21 (CDKN1A): molecular mechanisms and relevance in chemical toxicology. *Arch Toxicol* 2015; 89 (2): 155–178.
31. Hauge S, Macurek L, Syljuasen RG. p21 limits S phase DNA damage caused by the Wee1 inhibitor MK1775. *Cell Cycle* 2019; 18 (8): 834–847.
32. Elbaek CR, Petrosius V, Sorensen CS. WEE1 kinase limits CDK activities to safeguard DNA replication and mitotic entry. *Mutat Res* 2020; 819–820: 111694.
33. Aarts M, Sharpe R, Garcia-Murillas I, Gevensleben H, Hurd MS, Shumway SD et al. Forced mitotic entry of S-phase cells as a therapeutic strategy induced by inhibition of WEE1. *Cancer Discov* 2012; 2 (6): 524–539.
34. Ghiasi N, Habibagahi M, Rosli R, Ghaderi A, Yusoff K, Hosseini A et al. Tumour suppressive effects of WEE1 gene silencing in breast cancer cells. *Asian Pac J Cancer Prev* 2014; 14 (11): 6605–6611.
35. Lewis CW, Jin Z, Macdonald D, Wei W, Qian XJ, Choi WS et al. Prolonged mitotic arrest induced by Wee1 inhibition sensitizes breast cancer cells to paclitaxel. *Oncotarget* 2017; 8 (43): 73705–73722.
36. Zheng H, Shao F, Martin S, Xu X, Deng CX. WEE1 inhibition targets cell cycle checkpoints for triple negative breast cancers to overcome cisplatin resistance. *Sci Rep* 2017; 7: 43517.
37. Cande C, Cohen I, Daugas E, Ravagnan L, Larochette N, Zamzami N et al. Apoptosis-inducing factor (AIF): a novel caspase-independent death effector released from mitochondria. *Biochimie* 2002; 84 (2–3): 215–222.
38. Lu HF, Chie YJ, Yang MS, Lee CS, Fu JJ, Yang JS et al. Apigenin induces caspase-dependent apoptosis in human lung cancer A549 cells through Bax- and Bcl-2-triggered mitochondrial pathway. *Int J Oncol* 2010; 36 (6): 1477–1484.

39. **Zhao YX, Sun ZF.** [Molecular mechanisms of chemoresistance in head and neck squamous cell carcinoma]. *Lin Chung Er Bi Yan Hou Tou Jing Wai Ke Za Zhi* 2017; 31 (11): 888–891.
40. **Thaker PH, Han LY, Kamat AA, Arevalo JM, Takahashi R, Lu C et al.** Chronic stress promotes tumor growth and angiogenesis in a mouse model of ovarian carcinoma. *Nat Med* 2006; 12 (8): 939–944.
41. **Guo K, Ma Q, Wang L, Hu H, Li J, Zhang D et al.** Norepinephrine-induced invasion by pancreatic cancer cells is inhibited by propranolol. *Oncol Rep* 2009; 22 (4): 825–830.
42. **Celik E, Kaplan HM, Singirik E.** The impact of propranolol on apoptosis in cutaneous squamous cell carcinomas. *Bratisl Lek Listy* 2020; 121 (11): 801–804.
43. **Devarajan E, Sahin AA, Chen JS, Krishnamurthy RR, Aggarwal N, Brun AM et al.** Down-regulation of caspase 3 in breast cancer: a possible mechanism for chemoresistance. *Oncogene* 2002; 21 (57): 8843–8851.
44. **Yang S, Liu J, Thor AD, Yang X.** Caspase expression profile and functional activity in a panel of breast cancer cell lines. *Oncol Rep* 2007; 17 (5): 1229–1235.
45. **Cregan SP, Dawson VL, Slack RS.** Role of AIF in caspase-dependent and caspase-independent cell death. *Oncogene* 2004; 23 (16): 2785–2796.
46. **Liao X, Che X, Zhao W, Zhang D, Bi T, Wang G.** The beta-adrenoceptor antagonist, propranolol, induces human gastric cancer cell apoptosis and cell cycle arrest via inhibiting nuclear factor kappaB signaling. *Oncol Rep* 2010; 24 (6): 1669–1676.
47. **Anding AL, Chapman JS, Barnett DW, Curley RW, Jr., Clagett-Dame M.** The unhydrolyzable fenretinide analogue 4-hydroxybenzyl-retinone induces the proapoptotic genes GADD153 (CHOP) and Bcl-2-binding component 3 (PUMA) and apoptosis that is caspase-dependent and independent of the retinoic acid receptor. *Cancer Res* 2007; 67 (13): 6270–6277.
48. **Block I, Muller C, Sdogati D, Pedersen H, List M, Jaskot AM et al.** CFP suppresses breast cancer cell growth by TES-mediated up-regulation of the transcription factor DDIT3. *Oncogene* 2019; 38 (23): 4560–4573.
49. **Mihailidou C, Papazian I, Papavassiliou AG, Kiaris H.** CHOP-dependent regulation of p21/waf1 during ER stress. *Cell Physiol Biochem* 2010; 25 (6): 761–766.
50. **Jauhainen A, Thomsen C, Strombom L, Grundevik P, Andersson C, Danielsson A et al.** Distinct cytoplasmic and nuclear functions of the stress induced protein DDIT3/CHOP/GADD153. *PLoS One* 2012; 7 (4): e33208.

Received November 3, 2022.

Accepted November 14, 2022.